# Comparison of Measurements of Atmospheric Wet Delay by Radiosonde, Water Vapor Radiometer, GPS, and VLBI

A. E. NIELL

*MIT Haystack Observatory, Westford, Massachusetts*

A. J. COSTER

*MIT Lincoln Laboratory, Millstone Radar, Lexington, Massachusetts*

F. S. SOLHEIM

*Radiometrics Corporation, Boulder, Colorado*

V. B. MENDES, P. C. TOOR, AND R. B. LANGLEY

*Geodetic Research Laboratory, University of New Brunswick, Fredericton, New Brunswick, Canada*

C. A. UPHAM

*MIT Lincoln Laboratory, Millstone Radar, Lexington, Massachusetts*

(Manuscript received 9 March 2000, in final form 17 August 2000)

## ABSTRACT

The accuracy of the Global Positioning System (GPS) as an instrument for measuring the integrated water vapor content of the atmosphere has been evaluated by comparison with concurrent observations made over a 14-day period by radiosonde, microwave water vapor radiometer (WVR), and Very Long Baseline Interferometry (VLBI). The Vaisala RS-80 A-HUMICAP radiosondes required a correction to the relative humidity readings (provided by Vaisala) to account for packaging contamination; the WVR data required a correction in order to be consistent with the wet refractivity formulation of the VLBI, GPS, and radiosondes. The best agreement of zenith wet delay (ZWD) among the collocated WVR, radiosondes, VLBI, and GPS was for minimum elevations of the GPS measurements below 10°. After corrections were applied to the WVR and radiosonde measurements, WVR, GPS, and VLBI (with 5° minimum elevation angle cutoff) agreed within ~6 mm of ZWD [1 mm of precipitable water vapor (PWV)] when the differences were averaged, while the radiosondes averaged ~6 mm of ZWD lower than the WVR. After the removal of biases between the techniques, the VLBI and GPS scales differ by less than 3%, while the WVR scale was ~5% higher and the radiosonde scale was ~5% lower. Estimates of zenith wet delay by GPS receivers equipped with Dorne–Margolin choke ring antennas were found to have a strong dependence on the minimum elevation angle of the data. Elevation angle dependent phase errors for the GPS antenna/mount combination can produce ZWD errors of greater than 30 mm over a few hour interval for typical GPS satellite coverage. The VLBI measurements of ZWD are independent of minimum elevation angle and, based on known error sources, appear to be the most accurate of the four techniques.

## 1. Introduction

The atmosphere is of great importance to all living things on the earth, at times to be enjoyed and at other times to be deplored. However, to space geodesists who use the Global Positioning System (GPS) and Very Long Baseline Interferometry (VLBI) to make high-accuracy measurements of the solid earth it is always a nuisance.

On the other hand, because their measurements are affected by the atmosphere, geodesists are able to estimate those properties to which their observations are sensitive. Among these are the vertically integrated delay of the radio signal due to water vapor in the atmosphere. Because of the importance of water vapor to meteorology, the prospect of a new, relatively inexpensive instrument to determine its spatial and temporal distribution should be welcomed (Bevis et al. 1992; Businger et al. 1996).

The operational tool for determining the distribution of water vapor in the atmosphere has been the radio-

*Corresponding author address:* Dr. Arthur E. Niell, MIT Haystack Observatory, Westford, MA 01886.
E-mail: aniell@haystack.mit.edu

sonde (Westwater 1997). Radiosondes provide vertical profile information about the meteorological variables pressure ($p$), temperature ($T$), and relative humidity (RH), but the operational cost restricts their use by the National Weather Service (NWS) and most other national agencies to only twice per day.

GPS, VLBI, and most water vapor radiometers (WVRs) that are in current use directly measure only the integrated properties of the atmosphere. These instruments are able to determine departures from spatial homogeneity of the water vapor distribution through azimuth- and elevation-dependent residuals of the observables to those expected for a homogeneous atmosphere (Alber et al. 1997; Bar-Sever et al. 1998; Chen and Herring 1997). With sufficient density of antennas, tomography of spatial variations is possible, but for economic reasons this is likely to be practical only for GPS. A WVR with temperature and water vapor profiling capability has also been developed (Solheim et al. 1998). Although it does not have the vertical resolution of a radiosonde, it has the advantage of high temporal resolution and is able to detect cloud liquid water.

The primary advantage of VLBI, GPS, and WVR is the almost continuous measurement that is possible. Although the expense of VLBI and WVR systems is an impediment to their use in an operational network, the currently planned surface spatial density of GPS antennas will be much higher than for the radiosonde network and does offer a significant addition to the meteorological observing program. The potential value of ground-based GPS measurements of integrated atmospheric water vapor for meteorological purposes, such as proposed by Bevis et al. (1992), has been amply demonstrated (Kuo et al. 1993; Businger et al. 1996; Guo et al. 1999). The actual value of the GPS measurements for weather forecasting and for climate studies will depend on their accuracy and on the latency of the reported data. Radiosondes and GPS systems are complementary, but economics will determine the relative contribution of the various instruments.

For meteorologists, the accuracy standard for measurements of atmospheric water vapor has been the radiosonde, which is expected to produce values of integrated precipitable water vapor (PWV) with an uncertainty of a few millimeters. In order to evaluate the claims for accuracy and precision by each of the techniques, campaigns with collocated instruments are needed. Comparisons among GPS, WVRs, and radiosondes have been reported (Rocken et al. 1995b; Emardson et al. 2000), with agreement generally at the level of 1–2 mm of PWV, corresponding to 6–12 mm of zenith wet delay (ZWD). Since none of the comparisons included VLBI measurements at the time we initiated these observations, we took advantage of a planned VLBI observing campaign to schedule concurrent measurements over a 15-day period in August 1995 with all four systems: radiosonde, GPS, WVR, and VLBI (only four days). An expected result of this experiment was, in addition, direct and independent measurement of the spatial and temporal variability of water vapor in the vicinity of the Westford VLBI antenna. Since the primary goal of the VLBI campaign was the measurement of variations in the rotation of the solid earth (Clark et al. 1998), these results demonstrate an additional benefit of the VLBI measurement, that of independent assessment of atmospheric water vapor on a global scale.

The observations and analysis reported here differ in several respects from most previous reports. 1) The radiosondes used were Vaisala model RS-80 with the A-HUMICAP sensor, allowing a comparison with the VIZ sonde and analysis used by the NWS. 2) We were able to include the VLBI estimates of ZWD at a collocated site for comparison. 3) All of the GPS sites are geographically close (less than 50 km apart, including three within ~1 km), which allows investigation of systematic effects in the measurements. 4) For the GPS measurements: (i) both antispoofing and selective availability were on, allowing an assessment of observations under the expected operating conditions for the foreseeable future; (ii) point positioning was used, thus removing the limitation of requiring a reference site; (iii) several different types of antenna mounts were utilized with the same type of antenna (Dorne–Margolin with choke ring), enabling evaluation of the effect of the near-field environment; (iv) two types of radome were used making it possible to see the effect of these types of radome on the measurement of water vapor.

While meteorologists traditionally deal with precipitable water vapor as the integrated measurement from radiosondes, this quantity is not uniquely provided by the other three techniques since the distribution of temperature and water vapor along the ray path are not known. Rather it is the integral of the index of refraction of water vapor through the atmosphere that is determined. [Delay is measured directly by VLBI and GPS but is a derived quantity for WVR, based on the native measurement of brightness temperature and calibration by radiosondes (see section 2b).] Since this quantity is directly calculable from the radiosonde profiles by ray tracing, we have chosen to evaluate the relative performance of the instruments through measurements of the excess electrical path length through the atmosphere, compared to the vacuum distance. This additional path length is usually referred to as a "delay," with the conversion factor assumed to be the vacuum speed of light. The measure of water vapor used by meteorologists, precipitable water vapor, is measured directly only by radiosonde, and an additional error would be introduced into the other three techniques in order to make the comparison using PWV.

In this paper we report comparison and evaluation of measurements of the zenith wet delay. Periods of obvious atmospheric inhomogeneity were seen, but the ability of GPS to measure such azimuthal asymmetries will not be discussed, except as it affects the accuracy of the zenith delays.
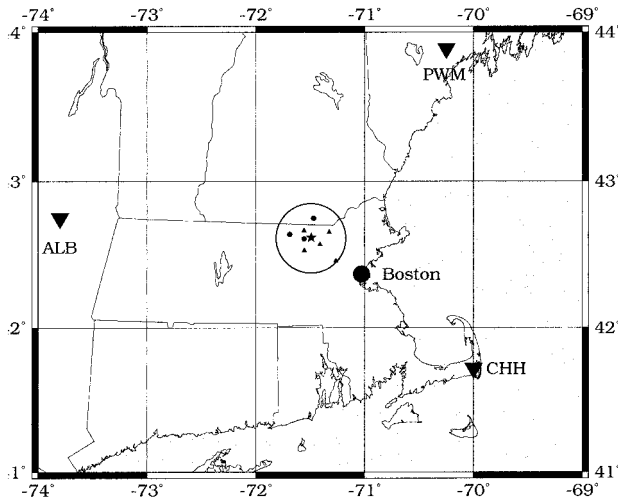
FIG. 1. Map of New England showing the locations of the GPS sites and of the NWS radiosonde launch sites (ALB, CHH, and PWM). The star represents the three GPS systems MHR0, WES2, and WFRD; they are too close to be distinguished. The small triangles represent (from top to bottom) SGJ0, ULWL, NVT0, AEN0, and G430. The small closed circles are at the locations of the GPS sites for which data were not used and represent (from top to bottom) TAC0, JIM1, and FIRE. The circle has a diameter of 50 km and is centered on the Westford sites. The Hanscom AFB radiosonde data were taken near the most southeast small triangle (G430).

The paper is organized as follows. In section 2 the experiment is described and necessary details of each technique are given. The definition of wet refractivity and its use is discussed in section 3. The accuracy of each technique is evaluated in section 4. The results for each type of measurement, their intercomparison, and the relationship of these results to those previously reported are described in section 5. In the final section recommendations derived from these measurements are given, and avenues for improvement are suggested.

## 2. Description of the observations

The observations to be compared were made 16–31 August 1995. Eleven GPS systems were distributed over an area within 25 km of the Haystack Observatory, Westford, Massachusetts (Fig. 1). The spatial coverage was chosen in order to be able to sample the water vapor distribution out to the distance as seen at an elevation angle of 5° from the Westford VLBI antenna at the observatory.

Three of the GPS systems, the WVR, the VLBI antenna, and the radiosonde launches were concentrated within approximately 1 km of each other. This allowed comparison on a spatial scale within which the water vapor distribution should be highly correlated at the level of accuracy of these instruments. Furthermore, the three GPS systems used the same receiver and antenna types in order to evaluate the consistency of the measurements by nominally identical systems. One of the three is WES2 (also known as WEST), which is an International GPS Service (IGS) site. The other eight GPS systems were located at sites chosen for their availability and field of view (horizon mask). The locations and types of receivers are given in Table 1.

The observations are shown in Fig. 2 and described in the following sections.

### a. Radiosondes

Vaisala RS-80 radiosondes were launched twice daily within one hour of the scheduled radiosonde flights of the NWS. Because of restriction by the Federal Aviation Administration to launch only during daylight hours, the sondes were released primarily within 10 min of 1110 and 2310 UTC. In a few days, an additional sonde was launched near 1710 UTC. Only pressure, temperature, and relative humidity were received from the local sondes; no wind information was obtained. Prior to launch, the calibration provided with the sonde was read from paper tape. The signal transmitted from the sonde was recorded at the full rate of once per second, using equipment provided by Vaisala. The sondes typically took approximately 90 min to rise to a pressure level of ~30 hPa and another 30 min to fall to the point that tracking was lost (~900 hPa). [Although the descending

TABLE 1. GPS site location and equipment.

| Site | Location | Receiver* | Antenna** | Barometer |
|------|----------|-----------|-----------|-----------|
| AEN0 | Harvard, MA | AOA | DMCR | Paroscientific |
| FIRE | Groton, MA | Ashtech | 718B | — |
| G430 | Lincoln Laboratory, Lexington, MA | AOA | DMCR | Vaisala |
| JIM1 | Townsend, MA | Ashtech | 718B | — |
| MHR0 | Haystack Observatory | AOA | DMCR | Rainwise |
| NVT0 | Nashoba Technical High School, Westford, MA | Ashtech | DMCR | — |
| SGJ0 | Pepperell, MA | AOA | DMCR | Paroscientific |
| TAC0 | Nashua, NH | AOA | DMCR | Rainwise |
| ULWL | University of Lowell, Lowell, MA | Ashtech | DMCR | Vaisala |
| WES2 | Haystack Observatory | AOA | DMCR | Setra |
| WFRD | Haystack Observatory | AOA | DMCR | — |

\* AOA—Allen Osborne Associates SNR-800 TurboRogue receiver; Ashtech—Z-XII receiver.
\*\* DMCR—Dorne–Margolin antenna with choke ring. For the Ashtech Z-XII this antenna is model number 700936, and observations were made with the included radome. Of the AOA sites, only WFRD had a radome (see text). 718B—Ashtech 700718B antenna.
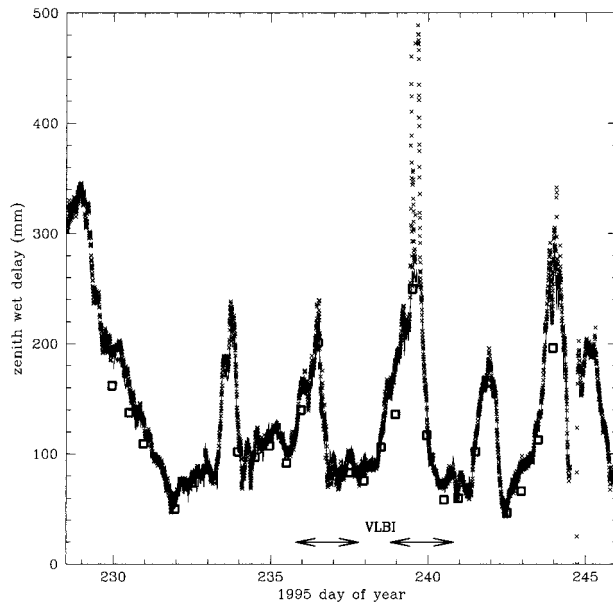
FIG. 2. Uncorrected and unedited zenith wet delays as measured by WVR (×), GPS (solid line) and Vaisala RS-80 L15 A-HUMICAP radiosonde (open square). Corrections for the WVR and radiosonde data are discussed in sections 3 and 4a, respectively. The arrows indicate the periods for which VLBI data were compared.

relative humidity measurement sometimes agreed with the ascending data within 10%–20%, the differences were often much larger. Nash and Schmidlin (1987) attribute this to icing of the sensor at the highest levels, leading to invalid results as the sonde descended.] After deleting those data recorded both prior to launch and after the sonde passed the 50-hPa level ascending, the remainder was smoothed and decimated by using a quadratic fit to 20 s of data centered on multiples of 60 s. This filtering gave a vertical resolution near the surface of ∼200 m. Geopotential heights were calculated using the hypsometric equation (e.g., Wallace and Hobbs 1977, p. 55). Comparison of the height calculation for profiles from the NWS gave agreement of better than 20 m at pressures less than 100 hPa (and much better at higher pressures).

The zenith wet delay was calculated for each radiosonde profile with a ray trace program (Niell 1996) that assumes that the measured pressure, temperature, and dewpoint depression were obtained along a vertical ascent (although the horizontal motion of almost all radiosonde trajectories is significant). Since this same program was employed in creating the mapping functions used to estimate the atmosphere delays for both the GPS and VLBI analysis (Niell 1996), the possibility of error due, for example, to the use of different physical constants is reduced (see section 5).

### b. Water vapor radiometer

A Radiometrics WVR-1100 two-frequency radiometer was mounted on a 15-m tower approximately 200

m from the site MHR0 and 625 m from the radiosonde launch site. Data were taken continuously in a series of tip curves consisting of sequences at nine elevations from −14.9° through zenith to +14.9° at four equally spaced azimuths from 0° to 135°. Opacities were calculated from the brightness temperatures measured by the WVR using the radiative transfer software of the National Oceanic and Atmospheric Administration (NOAA) Wave Propagation Laboratory (Schroeder and Westwater 1991). Retrieval coefficients for converting the opacities to ZWD were obtained by regression of the opacities and ZWD calculated from radiosondes for each of the NWS sites of Albany, New York (ALB), Chatham, Massachusetts (CHH), and Portland, Maine (PWM) for the months of August and September for the preceding four years (see Elgered 1993 for details). [PWM was replaced by nearby Grey, Maine (GYX) in September 1994. As a consequence, the radiosonde comparisons described in this paper use the data from GYX.] The opacities were calculated using the radiative transfer software of the NOAA Wave Propagation Laboratory (Schroeder and Westwater 1991). The coefficients obtained from the ALB radiosonde data were adopted for the conversion of opacity to ZWD. Using either of the other retrieval coefficients would have changed the ZWDs by less than 0.5%.

The nine-elevation-angle tip-curve sequence resulted in an estimate of the ZWD every 5 min. The WVR ran continuously from 12 August to beyond the end of the experiment. The only loss of data occurred because of a power outage on one day. The measured ZWDs are shown in Fig. 2.

A shortcoming of most WVRs for the measurement of ZWD is the deleterious effect of rain or of condensation of water on the optics, which causes the brightness temperatures to be in error. This is illustrated by the extremely high values of ZWD during periods of rain, such as on day of year (DOY) 239. Estimates of liquid water are also calculated by the WVR, but these do not allow sufficiently reliable editing of the ZWD data to be able to remove values contaminated by liquid water on the optics. For the duration of this experiment, the editing of the WVR data to reduce the amount of contaminated data was based both on the liquid water estimates and on sudden changes in the brightness temperatures of both radiometer channels (Elgered et al. 1991). In order to assess the intrinsic accuracy relative to the other techniques, not the operational difficulties, only those values not corrupted by rain are included in all comparisons described below.

### c. GPS

All GPS receivers were either Allen Osborne Associates (AOA) SNR-8000 TurboRogue or Ashtech Z-XII. Two of the Ashtech receivers were connected to Ashtech 700718B (Geodetic III) antennas, while the other nine

receivers used the Dorne–Margolin antenna with choke rings as sold by AOA and by Ashtech (model 700736B).

The GPS ionosphere-free phase data were analyzed using GPS Inferred Positioning System/Orbit Analysis and Simulation Software (GIPSY/OASIS-II) in the point positioning mode (Zumberge et al. 1997) with scripts based on xt-gipsy scripts (Webb and Zumberge 1995). The receivers were set to sample the data streams every 30 s, and the recorded data were decimated to 300 s in the analysis. Two features were added: 1) the mapping function was changed from the Lanyi mapping function (Lanyi 1984), which was the default in GIPSY at the time of the analysis, to the Niell Mapping Function (NMF) (Niell 1996); and 2) the a priori zenith troposphere delays were calculated from accurate surface pressure measurements so that the zenith troposphere correction, estimated using the NMF wet mapping function as the partial derivative, is the zenith wet delay. Although the Lanyi mapping function has the potential to be more accurate if the upper atmosphere can be appropriately characterized (tropopause height, lapse rate, height of isothermal layer beginning at the surface, and surface temperature), NMF was chosen because of its higher accuracy and precision in the absence of this effort (see, e.g., Mendes 1999) and because no surface meteorology is required for its implementation. In order to ascertain the error in the estimation of ZWD incurred by using the analytical mapping functions, both the hydrostatic and the wet mapping functions were also calculated from the radiosonde profiles using ray tracing (Niell 1996). (See section 4c for details.) During this period the largest error (that is, the largest difference relative to that which would be obtained from the ray trace of a radiosonde profile) in estimated zenith delay for either the hydrostatic or wet mapping functions is ~2.5 mm.

For each site the data were analyzed separately for each UTC day. Satellite final orbits and clocks were obtained via file transfer protocol from the Jet Propulsion Laboratory (JPL). Initially the site position, troposphere corrections, and receiver clock values were estimated for each day. The troposphere delay was treated as a random walk stochastic parameter with a variance per unit time of $(1 \text{ cm h}^{-1/2})^2$. This value is within 10% of the median value for this area as determined from 61 geodetic VLBI experiments in the period 1987–91 (Niell 1996). The clocks were estimated as white noise for each epoch. The ZWD was estimated two ways. First, the variation of the troposphere was determined when the site position was also estimated. Then the position was fixed to the average of the estimated values, and only the zenith troposphere delays and receiver clocks were estimated. The impact on estimated ZWD is discussed in section 4d(5).

A system noise of 1 cm was assumed for each data point. An estimate of goodness of fit, $\chi^2$ per degree of freedom, is generated for each solution. For all sites the value varied from ~0.7 for the 5° cutoff to ~0.25 for the 30° cutoff, indicating that the formal uncertainties in the estimated parameters should be decreased by approximately 20%–50%. However, these uncertainties do not take into account systematic effects such as satellite orbit errors (section 4d) or errors in the atmosphere mapping functions (section 4c).

Some analysts use an elevation-dependent weighting function for the delays in order to reduce the sensitivity to the low elevation-angle data (e.g., Collins and Langley 1999). This would be appropriate if the larger residual scatter at low elevations were due only to larger errors in the observables. Although the delay observables do have lower signal-to-noise ratio at low elevations, the postfit residuals are much larger than the observable error and are dominated by scattering and multipath. Therefore, we have used uniform weighting in order to investigate the actual effect on the estimation of the modeling errors.

During the observing period, both antispoofing and selective availability were on for most satellites.

### d. VLBI

The Westford 18-m antenna was one of five VLBI antennas that observed continuously for 5 days to study the repeatability of geodetic measurements, including relative site locations and earth orientation parameters. (Only 4 days of data were successfully observed with the Westford antenna.) The other antennas were in Fairbanks, Alaska; Kokee, Hawaii; Ny Alesund, Norway; Onsala, Sweden; and Wettzell, Germany. The observations are part of the National Aeronautics and Space Administration (NASA) Space Geodesy Project.

Analysis of the observations followed the procedures described in Niell (1996). Briefly, the estimated parameters were the site positions (except for Gilcreek, which was held fixed), the stochastically varying clocks and wet troposphere delays for each site, and two nutation parameters. It was possible to estimate only the zenith wet delay since the hydrostatic delay used as the a priori value was based on measured pressure at the site. In order to be consistent with the GPS analysis for the Westford estimates, the hydrostatic zenith delays were calculated from the same barometric pressure measurements used for the GPS analysis but were corrected to the intersection of axes of the VLBI antenna.

The average random walk stochastic parameter for the atmosphere variation at Westford for the four VLBI experiments was 0.4 ps² s⁻¹, with values ranging from 0.2 to 1.5 ps² s⁻¹. These are consistent with the values seen for summer months in the 1987–91 VLBI data (Niell 1996). Bar-Sever et al. (1998) found that improvement in repeatability could be obtained by tuning this parameter for the GPS analysis, but they were limited to characterizing their entire dataset by one value. For VLBI the value is obtained separately for each 24-h experiment from the delay rate data (Herring et al. 1990).

### e. Surface meteorology

Accurate barometric pressure must be used to calculate the zenith hydrostatic delay through the atmosphere in order to estimate the best value for the ZWD. The sensitivity of the hydrostatic delay to pressure error is $\sim 2$ mm hPa$^{-1}$, so that an accuracy of $\sim 0.1$ hPa will insure that the error in hydrostatic delay is not significant in the measurement of the wet delay. Since the mapping functions used do not make use of surface meteorology, relative humidity and temperature are not needed for the GPS and VLBI measurements of ZWD.

The primary pressure sensors for the experiment were two Paroscientific barometers, models 740-16B and 1016B. The quoted accuracy for both is better than 0.1 hPa for the pressures experienced during these observations. The two barometers agreed to better than 0.005 hPa at every opportunity for comparison, including before, after, and several times during the experiment. The model 740-16B had a digital display and was used to calibrate the barometers at other sites (Table 1).

For any site without a barometer the differential pressure from that GPS antenna to the barometer at a site with accurate pressure data was calculated using the height difference as determined by the GPS data and an assumed lapse rate of 6 K km$^{-1}$. This differential pressure was added to the accurate value from the Paroscientific barometer. The largest height difference was 80 m over a horizontal distance of less than 20 km. By making this comparison between the two spatially separated Paroscientific barometers, we verified that the error in the calculated pressure was less than 0.1 hPa. For those sites having barometers, the pressure correction from the location of the barometer to the GPS antenna was measured with the Paroscientific barometer.

## 3. Wet refractivity

The ZWD is the integral of the water vapor refractivity through the atmosphere in the zenith direction. The wet refractivity, $N_w$, used in our data analysis is given by Davis et al. (1985) as

$$N_w = \left( k_2 \frac{e}{T} + k_3 \frac{e}{T^2} \right) Z_w^{-1},$$

where $e$ is the water vapor pressure (in hPa), $T$ is the temperature in kelvins, $k_2 = 64.79$ K hPa$^{-1}$, $k_3 = 377$ 600 K hPa$^{-1}$, and $Z_w^{-1}$ is the inverse compressibility, which has a value that differs from 1 by less than 0.1%. By including the $e/T$ term with the refractivity due to the majority of other constituents of the atmosphere, Davis et al. (1985) partitioned the atmosphere delay into hydrostatic delay, calculable with approximately 0.02% accuracy from the surface pressure, and "wet" delay. The refractivity of the "wet" component, $N_w'$, is given by

$$N_w' = \left( k_2' \frac{e}{T} + k_3 \frac{e}{T^2} \right) Z_w^{-1}$$

where $k_2' = 17$. Davis et al. (1985) suggested using uncertainties of 10 and 3000 for $k_2$ and $k_3$, respectively, to reflect the experimental uncertainties. These result in an uncertainty of 1% in $N_w$, and thus in the ZWD as calculated by ray tracing the radiosonde profiles.

Bevis et al. (1994) reassessed the refractivity constants and arrived at slightly different values and uncertainties. However, the resulting wet refractivity differs by much less than 1% from that of Davis et al. (1985) for typical meteorological conditions. The uncertainty Bevis et al. arrived at is somewhat smaller, $\sim 0.4\%$.

The use of hydrostatic and wet delays as defined by Davis et al. (1985) and incorporated by Bevis et al. (1994) results in an error of $-3.3 \pm 0.1\%$ in the estimated wet delay. This is due to the inclusion of part of the $e/T$ term in the refractivity of the hydrostatic component of the delay. However, the total delay, obtained by combining the hydrostatic and wet delays, is not biased if accurate surface pressure has been used for the a priori hydrostatic zenith delay. When comparing measurements of wet delay and integrated precipitable water vapor by different techniques or from different sources, it is important to be consistent in the use of the constants. Bevis et al. (1994) does correctly compensate for the error in wet delay in their conversion to PWV.

The WVR retrieval coefficients were calculated, as described in section 2b, using the full wet refractivity (i.e., using $k_2$ rather than $k_2'$). In order to be consistent with the analysis of the VLBI, GPS, and radiosonde measurements, the measured WVR values used in the comparisons from these experiments have been reduced by 3.3%. While this is not exactly equivalent to determining the regression coefficients with the consistent refractivity, the remaining error is expected to be small compared to the correction, since the temperature variation is small where there is significant water vapor.

## 4. Error sources

A complete classification of the uncertainties of a system is multidimensional. In the time domain, the precision of a measurement may improve with the amount of observing time, but the error may increase if the accuracy degrades with time since the last calibration. The limited duration of this experiment allows evaluation and comparison of the four techniques up to only 14 days for the WVR, GPS, and radiosonde systems and to 5 days for the VLBI. Seasonal effects, which are likely (Liljegren et al. 1999), cannot be evaluated.

The uncertainty in the accuracy may also depend on the geometry of the observations. For the cases of GPS and VLBI, the precision of the ZWD estimates for characteristic times of order 20 min improves as data are included from lower elevation angles, but systematic errors on the timescale of a day, due to errors in the mapping functions, for example, will increase significantly when observations at elevation angles somewhere
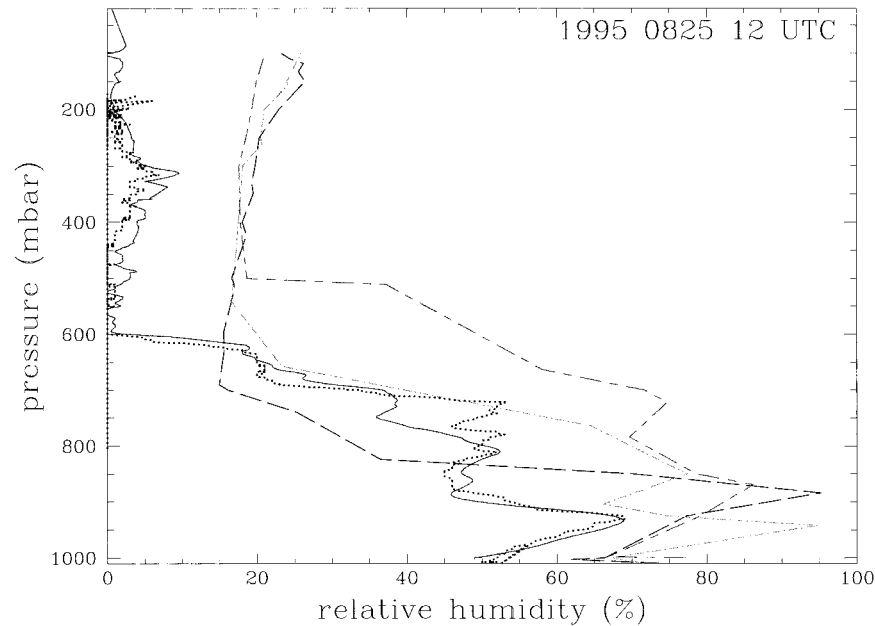
FIG. 3. Profiles of RH as a function of pressure for 1200 UTC 25 Aug 1995. No corrections have been made to these data. Solid line—Haystack Observatory; Dotted line—Hanscom AFB. The two sites are approximately 25 km apart. Both are from Vaisala RS-80 sondes. The NWS profiles are shown with symbols: ALB—long dash; GYX (PWM)—long dash/short dash; CHH—dash/dot.

below 10° are added to the solutions (MacMillan and Ma 1994).

In this experiment we are looking primarily for differences in the accuracies of the techniques. Each technique may have a bias in the measurements, and both the radiosondes and WVR are expected to have uncertainties in the scale of the ZWD estimates. Thus the initial model for the comparisons will consist of an offset and a scale difference between techniques. The significance of each of these estimated quantities must be evaluated in terms of the expected uncertainties of the measurements.

### a. Radiosonde

The accuracy of the Vaisala instrumentation is specified by the manufacturer to be better than 3% in RH, 0.2°C in temperature, and 0.5 hPa in pressure. In order to check the consistency of the sonde data at the time of launch, we compared for the period 1200 UTC 25 August through 2300 UTC 31 August the surface values of pressure and temperature from each sonde, with values measured at the launch site. The launch site pressure was obtained (as described above) from a barometer approximately 10 km away at the site SGJ0. The comparison temperature was measured at the site with a laboratory grade thermometer for which the readout uncertainty was 0.5°C. The average difference (standard deviation), in the sense "sonde-before-correction minus site," was 0.0 hPa (0.7 hPa) and 0.0°C (0.7°C) for pres-

sure and temperature, respectively. These are similar to the differences of less than 1 hPa and less than 0.5°C found between Vaisala and VIZ radiosondes flown on the same balloons by England et al. (1993). Thus the characteristics of the sonde temperature and pressure sensors were consistent with the advertised values. However, for reasons that are not understood, when the measured difference between sensor and reference measurement were entered as corrections in the sonde receiver/processing unit, the temperatures recorded for the sondes were depressed by an average of 2.7°C (0.5°C). The recorded pressures differed from the reference pressures by −0.2 hPa (0.5 hPa). The effect of this temperature error is to increase the calculated ZWD by approximately 2% for the last half of the experiment, or 1% on average over the 14 days of data.

Unfortunately, the only local validation of relative humidity that was made was the following comparison. Fortuitously, the same model sonde, Vaisala RS-80 with the A-HUMICAP relative humidity sensor, was launched nearly simultaneously at Hanscom Air Force Base (AFB) near the GPS site G430 (Table 1) on 25 August 1995 at 1200 UTC. This allows an evaluation of the precision of the radiosonde sensors. The profiles of relative humidity versus pressure are shown in Fig. 3. Except for the feature near 700 hPa, the agreement in RH is better than 5%. This provides confidence in the precision of the sonde humidity measurements but not in accuracy, since the two sondes are likely to be subject to the same systematic errors.

Vaisala RS-80 A- and H-HUMICAP relative humidity sensors have been found to suffer from contamination by the packing material, which causes the relative humidity sensor to indicate lower values than are actually present (Liljegren et al. 1999). The error depends on the actual relative humidity and the time since construction and calibration of the sonde. Most progress in understanding and providing a correction has been made for the H-HUMICAP sondes. To evaluate the possibility that the difference seen for the sondes of the present study is due to this problem, two sondes that were not used in the 15-day experiment, but were from the same calibration batch, were taken to the Vaisala plant where the RH and temperature were compared to accurate sensors using a Vaportron. The accuracy of the Vaportron is ~1.5% in RH over the range 3%–97% and is 0.2°C in temperature. Five readings of RH from 0% to 90% were made at room temperature and pressure. A least squares fit indicated that the sonde read 0.90 times the reference value with a zero-point offset of −4% and a standard deviation of 2.6%. The temperature differed from the reference temperature by 0.3°C.

In order to determine if the symptoms were consistent with the hypothesis of contamination, one of the sondes was "baked out" at Vaisala and the relative humidity was measured again. The error in relative humidity was reduced, with the relative scale being 1.00, the zero-point offset −3%, and the standard deviation 1.2%. Thus, the sonde exhibited the expected recovery. Vaisala, in cooperation with the National Center for Atmospheric Research, has developed an algorithm for correcting both the H-HUMICAP and A-HUMICAP sondes. The data for 18–31 August were corrected by B. Lesht (1999, personal communication) using a proprietary algorithm based on the observed relative humidity and age since manufacture and calibration. The sonde ages ranged from 653 to 658 days, and the largest correction for pressures greater than 500 hPa was 3.8% (e.g., from 60.4% to 64.2% on 25 August). Comparisons among the different techniques described in section 5 use the corrected values of relative humidity.

To compare the radiosonde observations made at Haystack (HSTK) with those of the NWS, upper-air soundings from the three nearest sites (indicated in Fig. 1a) were obtained from the National Climatic Data Center. These sites are approximately equidistant (~150 km) from Haystack and sample three somewhat different environments. ALB (110 km to the east) is most like Haystack in being inland and at a height above sea level of ~80 m. CHH (180 km to the southeast) is at the end of Cape Cod, protruding into the Atlantic Ocean. GYX (formerly PWM; 130 km to the northeast) is a coastal site. However, unless Haystack is in an unusual climatological location, the average water vapor content at Haystack should be within the range of values of the three NWS sites.

Twice daily data from the three sites were obtained for the times of all corresponding Haystack launches
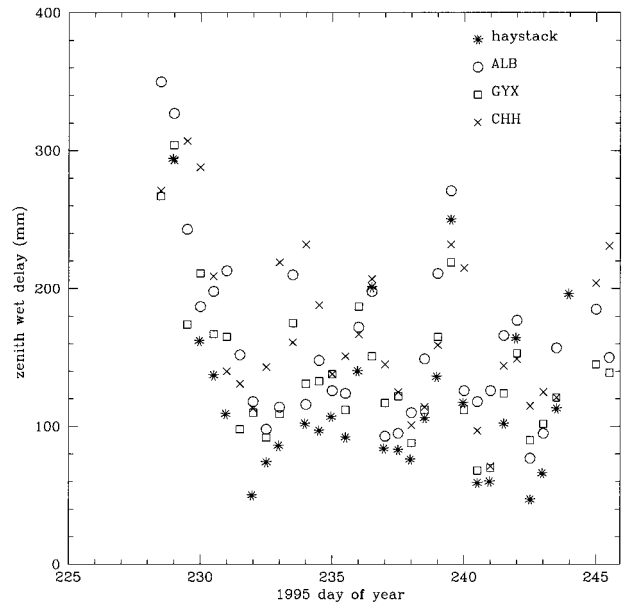


FIG. 4. Precipitable water vapor for the period 15–30 Aug 1995 from radiosonde measurements: Haystack—asterisk; ALB—circle; GYX (PWM)—square; CHH-×.

but the last. To the best of our knowledge the NWS sondes were the VIZ-B model, and the instrument outputs were analyzed by standard NWS procedures. The relative humidity at the mandatory and standard levels are shown in Fig. 3, at the same launch time as for the Haystack and Hanscom sondes described above. The ZWDs as measured at all four sites [HSTK (without the Vaisala correction), ALB, CHH, and GYX] are shown in Fig. 4 for the entire period. The Haystack/Vaisala values are clearly lower than the NWS/VIZ values, except for the four local maxima, when the Vaisala values are larger than about 160 mm. (There were no NWS data for the last Haystack/Vaisala point.)

Errors in the response and analysis of the VIZ sondes by NWS at low RH have been documented by Wade (1994), and for RH above 90% by Wade and Schwartz (1993) and by Westwater et al. (1989). As reported by Wade (1994) the apparent floor of the relative humidity values for the NWS/VIZ data for pressures less than ~700 hPa is due to 1) the NWS procedure of artificially setting the dewpoint depression to 30°C when the temperature goes below −40°C due to known nonlinearity in the RH sensor, and 2) using an incorrect value for the bias resistor in the sonde unit. For the profiles of 25 August at 1200 UTC (Fig. 3) the apparent water vapor for heights greater than 700 hPa for ALB contributes a delay of 17 mm, reducing the difference to only 4 mm of ZWD. This bias for the VIZ/NWS profiles, which occurs when the RH is very low (Fig. 4), accounts for at least part of the systematic difference. On this day there also appears to be a discrepancy for RH measurements at pressures greater than 700 hPa where the Vaisala sondes measure RH of ~50% while the VIZ

sondes record ~75%. This difference, seen independently in the Haystack and Hanscom profiles, is much larger than could be accounted for by the Vaisala contamination correction (~3%). However, because of the large distances between the launch sites, the significance of this difference cannot be assessed quantitatively.

Saturation of the Vaisala measurement at high relative humidity was observed on 27 August for the 1200 UTC flight. From 830 hPa down to 693 hPa the reading was 94% (the Vaisala correction is only 0.5% at this RH and level in the atmosphere). For that time, and for the previous flight at 0000 UTC, the NWS sites at ALB, CHH, and GYX recorded RH of 97%–99% in the same pressure range, thus supporting the observation by Wade and Schwartz (1993) that Vaisala measures too low by about 5% at high humidities.

Errors in the measurements of relative humidity and temperature are the main sources of error in the radiosonde measurements of ZWD. While the uncertainties given by Vaisala are 3% for RH and 0.2°C for temperature, it is apparent from the discussion above that the actual errors are larger.

### b. WVR

Uncertainty in the value of wet path delay measured by a WVR is due to 1) errors in the measurement of the brightness temperatures, 2) errors in the physical model for the atmosphere, 3) errors in the retrieval coefficients due to the difference in the atmospheric conditions at the time of the measurement from the average conditions used to derive the coefficients, and 4) errors in the retrieval coefficients due to errors in the radiosonde measurements.

The first three error sources are discussed by Solheim (1993). The instrumental noise and calibration errors of ~0.3 K contribute approximately 2 mm of ZWD uncertainty. The choice of physical model for the water vapor absorption results in an uncertainty of approximately 5%. This is corroborated by Cruz Pol et al. (1998), who find through noise simulations that the percentage error in the absorption coefficient for reasonable values of uncertainty in the radiometer brightness temperatures and in the radiosonde measurements ranges from ~2.5% at 23 GHz to ~8% at 32 GHz. Since opacity is proportional to the absorption coefficient and the regression is made on the opacity, the resulting uncertainty in ZWD is approximately 4%.

The mean radiating temperature of the atmosphere, $T_{MR}$, which enters the calculation of the opacities, is obtained from the radiosonde data when determining the retrieval coefficients for the WVR. Since the radiosonde data were restricted to the same time of year (August and September) as for the observations, the root-mean-square (rms) variation of $T_{MR}$ of 2.5 K contributes an uncertainty of 1% to the estimation of ZWD.

An integral component of the WVR analysis is the statistical determination of the retrieval coefficients from a large set of radiosonde data. To obtain enough radiosonde data from this geographical area it was necessary to use data from the NWS, which, as discussed above, have significant errors for dewpoint depressions greater than 30°, that is, low relative humidity at high altitude. However, England et al. (1993) showed, using Vaisala and VIZ packages, that this effect produces a negligible difference in the determination of the retrieval coefficients. On the other hand, systematic differences in the RH profiles at lower altitudes (less than 8000 m) may have an effect on the conversion of WVR brightness temperatures to delay.

The tests of Cruz Pol et al. (1998), cited above for evaluating the overall uncertainty of the WVR measurement, tested a random distribution of the contributing error source. However, the determination of retrieval coefficients by using radiosondes from only one manufacturer, which may thus be subject to common systematic errors, could introduce a systematic error in the WVR calibration. A particular example is the age-dependent scale error found in the Vaisala RS-80 radiosondes described in section 4a. If uncorrected, the error in measured relative humidity may be as large as 10%; Westwater et al. (1999) observed differences of 0.5 cm in 5 cm of integrated water vapor (corresponding to 30 mm difference in a total of 300 mm of ZWD) between two sets of nominally identical radiosondes used in measurements in February 1993.

How can such scale errors produce an error in the WVR retrieval coefficients? If the derived parameter, for example, ZWD, and the regressed parameters, for example, opacity at 23 GHz and 32 GHz, have the same functional dependence on the source of error, such as a scale error in the radiosonde relative humidity, then the coefficients of the opacities will be unchanged, and the bias error is negligible. ZWD and the primary term of the opacity are each proportional to the integral of the first power of water vapor density. However, the absorption coefficient of water vapor, which appears only in the opacity, has a second term that is proportional to water vapor density squared, with a maximum contribution of about 20% of the primary term (Staelin 1966). For an error in the measurement of water vapor of 10%, it is not unreasonable to expect departures from linearity in the ZWD–opacity relation of 2%–4%, corresponding to 5–10 mm of ZWD at the maximum observed in these experiments.

In order to evaluate the impact of this error, A. E. Niell and P. O. J. Jarlemark (unpublished manuscript) simulated the effect using 4 yr of Vaisala radiosonde data and the algorithms for estimating retrieval coefficients for the Atmospheric Sky Temperature Radiometer for Interferometric Delay Corrections (ASTRID) WVR (Elgered 1993). The retrieval coefficients for the WVR were first determined using the radiosonde data as recorded. The relative humidities were then multiplied by a factor of 0.8, corresponding to the difference between the Haystack/Vaisala sonde values and the NWS values

near the surface shown in Fig. 3, and the retrieval co-efficients were redetermined. The ZWDs were then re-computed from the brightness temperatures that were calculated from the original profiles, but using the sec-ond set of retrieval coefficients. In other words, the re-trieval coefficients were determined from profiles with a systematic error and used to estimate the ZWD from brightness temperatures that would have been observed by an ideal WVR. The differences are shown in Fig. 5 and are well fit by a simple quadratic function. At the maximum ZWD reported in this paper, 250 mm, the error would be ~6 mm. However, in a tropical region with a maximum ZWD as high as 400 mm, use of the same retrieval coefficients would result in an error of ~20 mm. The actual impact of this type of error is probably smaller for two reasons: 1) the average scale errors are only about half of the value used in the sim-ulation, and 2) the retrieval coefficients are usually de-termined from radiosonde data that span the range of conditions characteristic of the region in which the mea-surements are to be made. This problem is discussed further in section 5c, with respect to the current WVR–radiosonde comparison.

In summary, for the conditions of this experiment (20–250 mm of ZWD) and the uncertainties in the as-similation of radiosonde data for the regression coef-ficients, the resulting fixed and proportional components of the uncertainty in the measurements of ZWD for the Radiometrics WVR are 2 mm and 5%, or approximately 2–12 mm.

### c. Atmosphere errors in GPS and VLBI

GPS and VLBI are subject to the same errors from the atmosphere. The correction to the observed delay by the atmosphere is modeled as

$$\tau(e) = \tau_h^z m_h(e) + \tau_w^z m_w(e),$$

where $\tau_h^z$ is the a priori zenith hydrostatic delay (ZHD), $\tau_w^z$ is the estimated ZWD, and $m_h(e)$ and $m_w(e)$ are the hydrostatic and wet mapping functions. The wet delay is estimated from the observed delays after the best estimate of the hydrostatic delay has been subtracted. The zenith hydrostatic delay is from Saastamoinen (1972) as given by Davis et al. (1985), and the mapping functions are given by Niell (1996). NMF was chosen for the mapping functions because of the small biases and low seasonal error (Niell 1996; Mendes 1999), as well as for the simplicity of not requiring external input. At the same time the standard deviations of the mapping functions are comparable to mapping functions that do rely on surface meteorology.

Davis et al. (1985) carefully assessed the uncertainty in the calculation of the ZHD using the formula of Saas-tamoinen (1972). Taking into account uncertainties in the physical constants and in the calculation of the mean value of gravity, but not accounting for the error in surface pressure, the uncertainty is 0.5 mm. The sen-
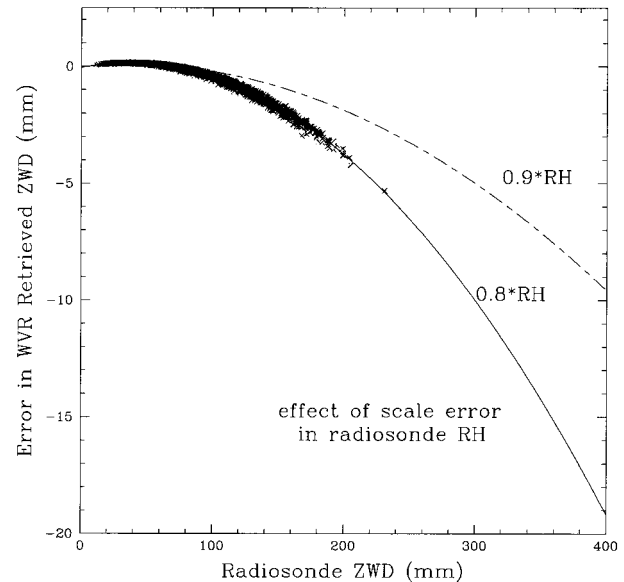


FIG. 5. The error in water vapor radiometer retrieval coefficient for fractional errors of 0.8 and 0.9 in RH in the radiosonde profiles used for determining the coefficients.

sitivity of the hydrostatic delay to an error in the mea-surement of surface pressure is 2.3 mm hPa$^{-1}$. The un-certainty in the pressure at the GPS antenna and at the intersection of axes of the VLBI antenna is less than 0.2 hPa. Thus, the combined uncertainty in the zenith hydrostatic delay is less than 1 mm. Because of the drought and lack of storm activity during this period, it is unlikely that nonequilibrium conditions resulted in errors greater than 1 mm (Hauser 1989).

Along with the ZWD, the site positions were also estimated. An error in the hydrostatic mapping function results in an error in the estimated height of a site of approximately one-third of the delay error at the lowest elevation angle (Niell 1996; MacMillan and Ma 1994) and in the estimated zenith atmosphere delay of ap-proximately −0.4 that of the height error. The uncer-tainty of the hydrostatic mapping function at 5° eleva-tion angle is approximately 0.01 (Niell 1996), so for the lowest elevation angle 24-h solutions, the uncertainty in the height is ~8 mm and the estimated ZWD is ~3 mm. At 15° the mapping function error for ZWD is negligible.

For the wet mapping function, the uncertainty at 5° elevation is 0.5% (Niell 1996), giving a maximum un-certainty of about 1 mm for the maximum ZWD of 250 mm for this period. The accuracy uncertainty due to errors in the calculation of the wet refractivity is ap-proximately 1% if based on the experimental uncer-tainties (Davis et al. 1985).

Within a day the value chosen for the allowed sto-chastic variation can affect the accuracy of the ZWD. If the characteristic time allowed by the stochastic pa-rameter is significantly longer than the actual time for a change in ZWD of a given magnitude, that is, if the

value of the stochastic parameter is too small, the estimated ZWD cannot change as rapidly as the actual ZWD. On the other hand, the geometric strength of the observations must be great enough to cause the estimate to follow the change. Under the conditions of these experiments, the data strength and the stochastic parameters are matched for VLBI and GPS solutions that include data to 15° minimum elevation angle or lower.

Several authors have demonstrated that including the estimation of gradients in the atmosphere improves the repeatability of site position (Bar-Sever et al. 1998; Chen and Herring 1997; MacMillan 1995). Bar-Sever et al. (1998) also indicated that the estimation of gradients improves the agreement of ZWD measured by GPS and WVR by 25%. However, it is not possible to determine whether the improvement in agreement is due to the inclusion of gradient estimation or to the reduction of the magnitude of the maximum postfit residual retained for the final of several iterations of parameter estimation. In either case the most significant improvement in agreement is due to lowering the elevation-angle cutoff angle from 15° to 7°. Our tests of the effect of including gradients in the VLBI estimation (section 4e) confirm the expectation that for an azimuthally symmetric distribution of observations, as obtained by the VLBI observing sequence, the inclusion of gradients has no effect on the mean value of the ZWD estimates.

### d. GPS

The accuracy of GPS measurements of position and zenith atmosphere delay are not limited by system receiver noise, but by modeling errors. These include satellite orbit errors, multipath and near-field scattering in the vicinity of the antenna, errors in the mapping functions used for the atmosphere delay estimation, treatment of the intrinsic antenna phase pattern, and the effect of a radome, if present. The sensitivity of results to these factors must be used to assess the lower limit of the accuracy of the measurements.

Zumberge et al. (1997) demonstrated that site positions determined from point positioning exhibit the same repeatability as if the site were included in a global solution. For a minimum elevation angle of 15° the vertical repeatability of 24-h solutions is on the order of 10 mm, corresponding to 3–4-mm uncertainty in the ZWD when both position and atmosphere (and receiver clock) are estimated. As discussed below (section 5a), the repeatability does not change significantly for lower elevation angle cutoff. Thus, in the absence of other systematic errors, the accuracy of GPS-determined ZWDs should be ~4 mm when averaged over 24 h. Evidence that this is not the case is described in section 5a.

1) ATMOSPHERE PARAMETERIZATION

As discussed in the previous section, the stochastic parameter is not expected to affect the estimates of the
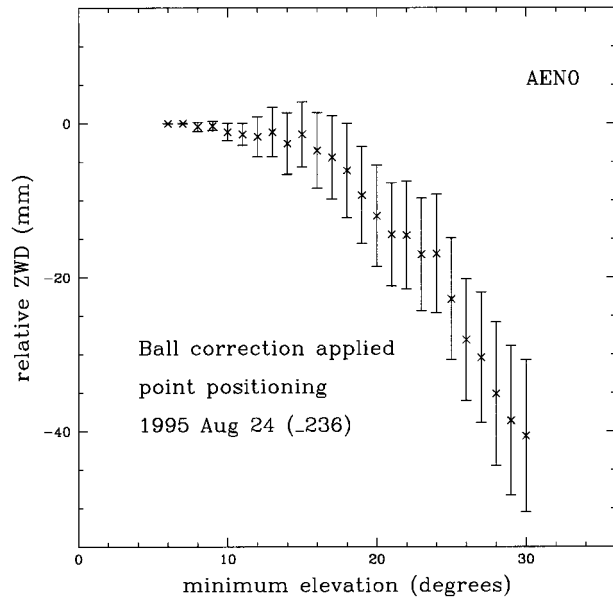


FIG. 6. Elevation-angle dependence of ZWD for AEN0 for 24 Aug 1995 after application of the Ball correction for the DMCR antenna. Compare to elevation-angle dependence in Fig. 7.

ZWD. The main effect is on the uncertainty in the estimates of the ZWD. However the formal errors also depend on the assumed value for the added phase delay noise. The formal errors for ZWD for the analysis utilized in this study are 2.7 mm, 3.6 mm, and 9.6 mm at 5°, 15°, and 30°, respectively.

2) ANTENNA PATTERN PHASE CORRECTION

The intrinsic electromagnetic properties of the Dorne–Margolin antenna and choke rings (DMCR) will result in a phase response that depends on the direction of the source of the signal. If the phase response is not the same in all directions, the estimated parameters, such as the position of the antenna and atmosphere delay, will be affected. The L1 and L2 phase patterns have been measured for several types of GPS antennas in an anechoic chamber by Schupler et al. (1994) and by Ball Brothers, Inc. (reported by Rocken et al. 1995a), with similar results. If the Ball phase corrections are applied to the antenna AEN0, the resulting estimated ZWDs have a dependence on the minimum elevation angle of the analysis that is shown in Fig. 6. As was done for the other analyses, the position of the antenna and the receiver clock are estimated also. Comparison with the elevation angle dependence of ZWD for AEN0 shown in Fig. 7 (note the vertical scale difference) demonstrates two problems with attempting to make a correction based on the chamber measurements. First, for any of the DMCR antennas used in the measurements reported here, the correction is much too large. That is, the dependence of estimated height on minimum elevation angle is significantly worse after application of the mea-
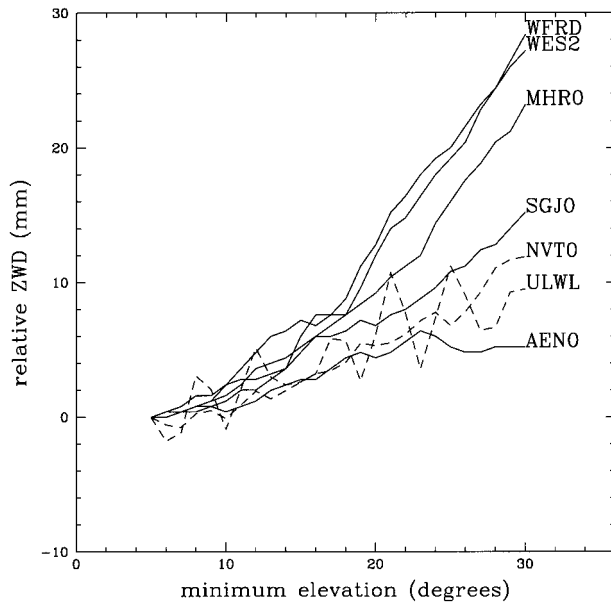
FIG. 7. Elevation-angle dependence of ZWD for different mounting types of the DMCR. The effect of the Ashtech radome has been removed from NVT0 and ULWL. WFRD has not been corrected for the effect of its radome. The relative ZWD at 30° would be reduced by ~15 mm, resulting in a dependence similar to SGJ0.

sured antenna pattern correction. If the chamber measurements are correct, then some other elevation-angle-dependent error source that is common to many sites has not been identified. Second, and perhaps more importantly, in view of the variation in elevation-angle dependence of height for different locations of the same type of antenna, no correction of the DMCR antenna pattern based on chamber measurement can be appropriate for all locations.

The point position results are not sensitive to the application of the Ball correction when determining the satellite orbits and clocks. Two global solutions were made using rinex files obtained from JPL for 32 sites. One solution included and one did not include application of the Ball correction for the DMCR antennas (only one antenna was not a DMCR). The position of the WES2 antenna, which was not included in the global solution, was then estimated using point positioning for both sets of the satellite clocks and orbits but without application of the Ball correction to WES2. The minimum-elevation dependence of the estimated height change with respect to the 5° minimum solution increased agreed within 10 mm. The total change in estimated height was 93 mm with the Ball-corrected orbits and 82 mm for the uncorrected orbits. The heights using the Ball corrected orbits were 80 mm larger for the 15° solutions.

Thus, since the systematic errors are made worse and there is no independent evidence that the chamber measurements are correct, no correction has been made for antenna phase errors.

### 3) EFFECT OF RADOME

The antenna type is the Dorne–Margolin antenna with choke rings. It is designated TurboRogue type T as supplied by AOA for use with the SNR-8000 and as model 700736B as supplied by Ashtech. The Ashtech antennas were covered with the radome provided by Ashtech. In the absence of a radome, antennas from the two manufacturers have been shown to give geodetic results that agree to 1 mm (Niell et al. 1996).

The introduction of any refracting substance between the antenna and the satellites will change the observed delay. This includes the addition of a radome or the unpredictable contamination by the collection of material on the antenna or radome, such as snow, leaves, or birds and their droppings. The addition of the Ashtech radome was shown by Niell et al. (1996) to produce an apparent change in height that decreased from +3 mm at 5° to −34 mm at 30°. The change is linear in elevation-angle cutoff angle, and the standard deviation about the linear fit is 2.5 mm. The corresponding error in average ZWD is from −1 to +14 mm, with a standard deviation of 1 mm. The error is smallest when data are included at the lowest elevation angles.

Other styles of radome will produce different errors, because of different geometry and refractivity of the radome material. For example, the 6-mm-thick, approximately 0.75-m diameter, hemispherical radome used on WFRD and on many of the concrete pillar monuments of the IGS produces an error in height that varies from +10 mm at 5° to −25 mm at 30° (Niell et al. 1996). It is unlikely that this error is due to the offset of the center of curvature of the radome from the phase center location of the antenna, since the refractivity of the radome material is not large enough to produce significant delay through radomes of thicknesses that are in use with GPS antennas.

These height errors due to the radome were determined from solutions that included estimation of the atmosphere delay. Thus, the approximate bias for ZWD estimates using a fixed antenna position and elevation-angle cutoff is obtained as −0.4 times the height error for the corresponding minimum elevation angle.

In addition to the error introduced by the radome itself, additional error may be incurred as matter accumulates on the radome. For example, the effect on height measurements of the accumulation of snow on the radome is documented by Jaldehag et al. (1996a). The equivalent change in ZWD for the errors observed during one month in January 1994 (50 mm in height) amounts to 20 mm.

### 4) ANTENNA MOUNT

An important result of these observations is the effect of the different types of antenna mounts on the geodetic and atmospheric delay estimates for the same antenna type. The characteristic of the estimated values that dif-

fered was their dependence on the minimum elevation angle of data included in the solution. Elósegui et al. (1995) first demonstrated this problem as it affects the geodetic results for WFRD, one of the sites discussed in this paper.

The support structures of the antennas varied greatly. Four were mounted on wooden tripods (ULWL and NVT0 on the flat roofs of commercial buildings; AEN0 and SGJ0 on peaked wooden roofs). MHR0 and WES2 were located on metal supports (MHRO on a 3-m pole; WES2 on a 10-m steel tower). WFRD, which is a FLINN-type monument, has a metal ring supporting the antenna over a marker plate on top of a 0.75-m diameter concrete pillar. The antenna is approximately 1.5 m above the ground. The remaining DMCR, G430, was mounted on a wooden platform 0.3 m above a flat roof. Because of difficulties with U. S. Customs, only a few days of data were obtained for the site TAC0, which is consequently not included in the analysis.

The dependence of estimated ZWD on minimum elevation angle, when the position is also estimated, is shown in Fig. 7 for seven of the eight DMCR antennas. An elevation-angle-dependent correction has been applied to the heights of ULWL and NVT0 to compensate for the effect of the Ashtech radome [see section 4d(3)]. On this figure, WFRD has not been corrected for the height error that is due to the radome in order to present the results for the FLINN-type monuments as they would be encountered in operation. The correction would decrease the ZWD at 30° by about 14 mm and put it in line with SGJ0.

The elevation-angle dependencies of the heights of the two non-DMCR antennas (FIRE and JIM1 are Ashtech 700718B antennas) are quite similar but are grossly different from those of the DMCRs. The apparent height for a minimum observed elevation angle of 30° reaches +200 mm compared to the height estimated with a 5° cutoff. (WES2, which has the largest change of the DMCR antennas, has a difference of −80 mm.) In this paper we will concentrate on the DMCR characteristics, and the 700718B will not be considered further.

5) FIXED HEIGHT

The estimates of the height of an antenna and of the troposphere delay are highly correlated. For the analysis used here, the zenith wet delay correction is approximately −0.4 times the change in the height correction. Of course, for measurements of ZWD for meteorological purposes, the position of the antenna should be fixed. In that case the apparent sensitivity of ZWD to minimum elevation angle is significantly reduced. It is apparent in the sense that, having chosen the height of the antenna, estimates of ZWD for different minimum elevations will not appear to change as much as when the position is also estimated. However, because of the correlation of height estimate and ZWD estimate, the mean value of the ZWD reflects the height chosen for the antenna. In the case of WES2, changing the height from that estimated for a minimum elevation angle of 30° to that of 5°, a difference of 8 cm, produces a mean difference in ZWD of 32 mm. Furthermore, since the actual phase error in the antenna has not been removed, the short-term errors in ZWD due to the change with time of the minimum elevation angle of the currently observed satellites are still present. Thus, both the accuracy and the precision of the ZWD estimation depend on the minimum elevation angle because of the elevation-angle-dependent antenna phase errors.

e. VLBI

Factors that contribute to errors in the estimate of the ZWD by VLBI are the observation noise, errors in the calculation of the a priori hydrostatic delay, errors in the hydrostatic and wet mapping functions, possible systematic elevation-dependent changes in delay, and errors due to unmodeled effects such as azimuthal asymmetry of the atmosphere delay. These affect the estimates of ZWD on different timescales. Errors in the constants in the calculation of the a priori ZHD result in a fixed fractional error for all troposphere delay estimates. The hydrostatic mapping function generally changes on a timescale of days. The observation noise and surface pressure measurements produce errors on a scale of minutes to hours.

The errors due to the atmosphere mapping functions and to the ZHD were described in section 4c.

The uncertainly of each ZWD estimate reflects the uncertainties in the observed delays and the value of the stochastic parameter describing the variability of the atmosphere delay (Herring et al. 1990). For the four days for which we have data, the average uncertainty in ZWD is 3.5 mm for the 5° minimum elevation angle solutions. The average uncertainty increases to 6.2 mm at 15° and to 18 mm at 30°.

Since estimates of all parameters should be independent of the minimum elevation angle of data included in the solution (within their uncertainties), a sensitive test for systematic errors is the elevation-angle cutoff test (Davis et al. 1985; Niell 1996). Although the estimates should be independent of the data included, the uncertainties in the parameter estimates will depend on minimum elevation. For ZWD, the uncertainty will increase with increasing minimum elevation angle for two reasons: there are fewer data and the geometric strength is reduced.

To evaluate the sensitivity of the ZWD estimates to minimum elevation angle for the VLBI analysis, two tests were made. First, the minimum elevation angle for Westford was incremented from 5° to 30° with the minimum elevation angle of the other antennas kept at 5°. The results are shown in Fig. 8, in which the averages of the differences of the ZWD estimates at the higher elevations are indicated at the minimum elevation angle of the included data. The error bars give the uncertainty
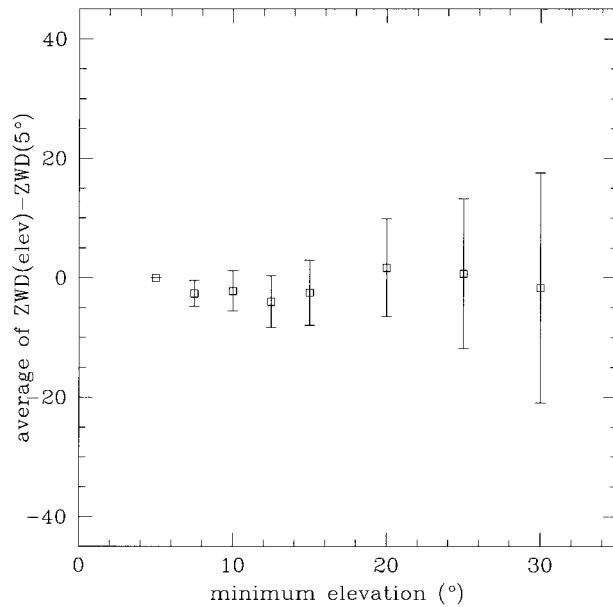
FIG. 8. Dependence of estimates of ZWD by VLBI on the minimum elevation angle of included data for the Westford site relative to the estimates at 5°. The error bars indicate the uncertainty in the difference with respect to the 5° solution.

diameter of Westford, thus sampling a cone through the atmosphere with half the diameter of that seen by Westford. The minimum elevation angle was 4.6° for the Westford antenna and 3° for the Haystack antenna. For 11 days of observations the mean difference of ZWD was 2.4 mm with a standard deviation of only 3.9 mm. The barometric pressure difference was correct to less than 1 hPa. Thus, VLBI determination of ZWD does not have discernible systematic errors and is consistent when measured by different systems.

To evaluate the effect of asymmetry of the atmosphere on the estimates of ZWD by VLBI, the solution for a minimum elevation angle of 5° was repeated twice more with stochastic variation in gradients in the atmosphere estimated at all sites with variances of approximately 10 ps at 12 h and 10 ps at 2 h. The average differences in estimated ZWD for the Westford VLBI site between the two gradient solutions and the nongradient solution were 0.6 and 1.0 mm, with standard deviations of 3 and 7 mm, indicating that any asymmetry in the atmosphere has a negligible effect on the accuracy of the zenith estimate.

Thus, with an estimated uncertainty in the absolute value of ZWD of less than 5 mm, VLBI appears to be the most accurate of the four techniques for measuring the delay through the atmosphere due to water vapor, although the subdaily precision appears to be larger than for WVR and GPS.

## 5. Results and comparisons

In many of the comparisons described in this section, the WVR is used as the common element because it operated continuously throughout the period (as did the GPS systems) and because it was located near the VLBI antenna, the radiosonde launch site, and several of the GPS systems. (This choice for the reference measurements does not indicate a judgment as to which instrument provides the best estimates of ZWD.) In comparisons with the WVR, data are excluded for all techniques during the periods when the WVR measurements were adversely affected by rain.

In all comparisons the WVR values have been reduced by 3.3% to make them consistent with the ZWD measurements of the other techniques. The Vaisala RS-80 data have been corrected with the Vaisala algorithm as applied by B. Lesht (1999, personal communication) and described in section 4a.

The mean values of the differences between the techniques are summarized in Fig. 9. The ZWDs determined by the WVR were subtracted from the ZWDs determined by VLBI, by GPS, and by the radiosondes launched at Haystack. The averages of the differences over the span of common data were then computed, excluding those intervals for which the WVR data suffered possible contamination by liquid water. For VLBI and for the WES2 GPS site, the ZWDs were interpolated to the time of the WVR measurement. The radiosonde

in the difference, which depends only on the number of observations not in common (Davis et al. 1985). There is no statistically significant change in the ZWD estimates with minimum elevation, in contrast to the GPS results (section 5a).

The second test was to change the minimum elevation angle of the other VLBI sites to 15° while keeping the Westford value at 5°. The average difference in ZWD at Westford is 1.3 mm with a standard deviation of 7.5 mm. Thus, from these two tests the estimates of ZWD by VLBI appear to be independent of the minimum elevation angle of the data.

The minimum elevation angle test is not sensitive to delay errors that are proportional to 1/sine(elevation) since such an error would be highly correlated with the ZWD estimate. If constant, such an error would appear as a bias in ZWD, while a varying error could not be distinguished from changes in ZWD. The most likely cause of such errors is associated with the motion of the antenna, due either to deformation of the antenna itself, or to changes in electrical path length of the cables with antenna orientation. A limit of less than 1 mm of ZWD can be set on this type of error due to the close agreement of the relative positions of the Westford and Haystack antennas (separated by 1.4 km) determined by VLBI and by conventional geodesy (Carter et al. 1980; Herring 1992).

An assessment of the accuracy of ZWD measurements by VLBI is available from a set of experiments in October–November 1989, in which both the Westford and Haystack antennas participated. The main difference in the two antennas is that Haystack is twice the
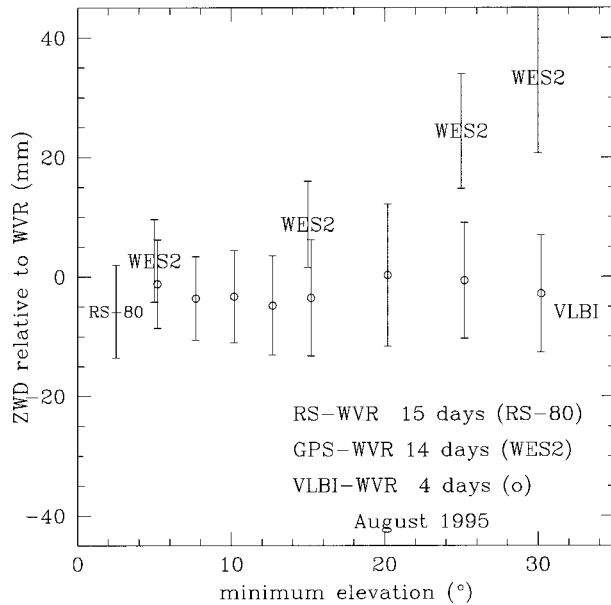
FIG. 9. The average differences of ZWD estimates by radiosonde, GPS, and VLBI relative to WVR. For GPS and VLBI, the dependence on minimum elevation angle is shown. The WVR values have been corrected to agree with the wet refractivity formulation of the GPS, VLBI, and radiosonde, as described in the text. The RS-80 radiosonde data have been corrected for packaging contamination by B. Lesht (1999, personal communication). For the Haystack radiosonde measurements, the indicated elevation angle is arbitrary. The error bars represent the standard deviations of the differences.
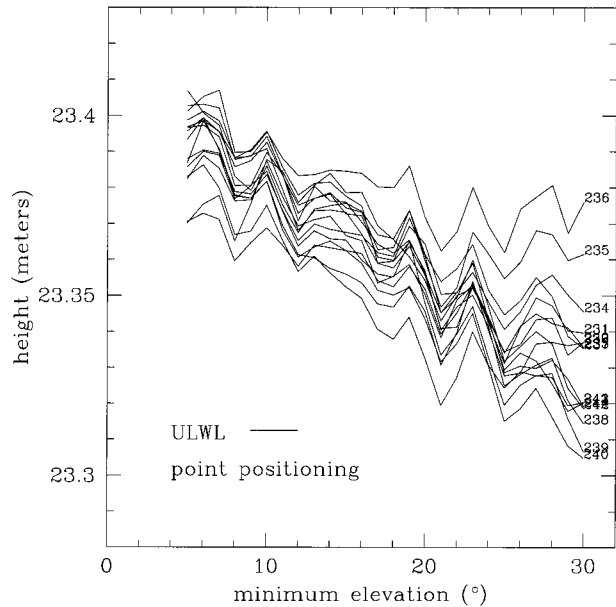


FIG. 10. The elevation-angle dependence of the radial component of ULWL as a function of minimum elevation angle for 14 days. For any minimum elevation, the scatter in height represents the variation that was observed over the 14 days of observation.

ZWDs were compared with the average of the WVR measurements obtained within 30 min following the radiosonde launch time, corresponding to the sonde traversing approximately the lower 7000 m of the troposphere. The VLBI and WVR differ by less than 3 mm when averaged over the entire period, regardless of the minimum elevation angle chosen for the VLBI analysis. The GPS observations, when all data are included down to a minimum elevation angle of 5° (i.e., all data that were retained at the time of the observations), also agree, on average, with the WVR results to within 3 mm. As the minimum elevation angle is increased, the mean difference increases, that is, the GPS analysis indicates more water vapor in the atmosphere, reaching more than 30 mm difference (~5 mm of PWV) when there are no satellites visible below 30° or data below this elevation angle are excluded.

The main points of this figure are to emphasize 1) the dependence of the GPS values on the elevation angle distribution of the data and 2) the independence of the VLBI measurements from such systematic errors.

This type of comparison is incomplete, however, since only the averages of the differences are shown, while the actual relation involves at least a scale factor as well as a bias. It is important to evaluate the scale differences because comparisons often use data spanning significantly different ranges of total water vapor. For example, the values of PWV reported by Westwater et al. (1999)

from the tropical western Pacific correspond to ZWDs that are almost disjoint with those evaluated in this paper. Their observations span the range ~250 to ~630 mm of ZWD, while ours ranged from ~50 to ~250 mm. Assuming the average ZWDs are 150 and 350 mm, a scale difference of 5% results in a bias difference of about 10 mm, or almost 2 mm, of PWV. It is also important to evaluate the character of the differences, whether bias or scale difference or both, in order to obtain information on the sources of the differences.

### a. GPS results

The day-to-day repeatability of ZWD can be estimated by looking at the height estimates, remembering the approximate conversion factor. The dependence of the radial coordinate of ULWL on minimum elevation angle for all 14 days is shown in Fig. 10. The standard deviation about the mean value, ~9 mm, does not change significantly for minimum elevations below 15° and is consistent with expected point positioning results reported by Zumberge et al. (1997). Thus, the day-to-day variation of ZWD for 24-h intervals, ~3–4 mm, should not be degraded by the inclusion of lower elevation-angle data, while their inclusion should improve the accuracy (or at least the agreement with VLBI).

Three of the GPS systems (WES2, WFRD, and MHR0) were, effectively, collocated since they were separated by less than 1.5 km. Over this distance the delay through the atmosphere is highly correlated. The expected difference in the zenith wet delay for this separation is on the order of a few millimeters, and the dry

TABLE 2. Calculated and observed mean ZWD differences (mm) between nearby GPS sites for 18–31 Aug 1995. The assumed scale height for the water vapor is 1500 m, and the mean ZWD is assumed to be 150 mm. The minimum elevation angle for the analysis was 5°.

|           | Expected (mm) | Observed (mm) | Std dev (mm) |
| --------- | ------------- | ------------- | ------------ |
| WFRD-WES2 | 2.9           | 0.9           | 4.4          |
| MHR0-WES2 | −2.8          | −4.4          | 6.1          |
| SGJ0-WES2 | 4.2           | 1.9           | 6.0          |
| WFRD-MHR0 | 5.7           | 5.2           | 6.5          |

fluctuations are expected to be much smaller (Treuhaft and Lanyi 1987). The differences in estimates of ZWD between these systems thus provide a measure of the precision of "identical" systems. On the other hand, comparisons of estimates by the same GPS system for different observing criteria, for example for different minimum elevations of the observations included in the solution, provide a lower limit for some of the systematic errors that affect the measurement of ZWD by GPS.

One indication of the level of agreement that can be obtained for ZWD estimates by independent GPS systems is the standard deviation of the differences between nearby systems. The three systems, WES2, WFRD, and MHR0, in addition to being spatially close, have very similar minimum elevation-angle dependencies (see Fig. 7), so their comparison will be indicative of the best that can be done in measuring ZWD from independent, but apparently similar, sites. The observed mean differences can be compared to an expected difference, obtained as follows. If the wet refractivity is assumed to decrease exponentially with a scale height, $H_{wv}$, of 1500 m (determined from the radiosonde profiles), and the average ZWD over the experiment is 150 mm, the expected ZWD difference between sites at height $h_1$ and $h_2$ is $150(h_1 - h_2)/H_{wv}$. The observed and expected differences for a minimum elevation angle of 5° are given in Table 2.

With a 5° elevation-angle cutoff, the ZWD for WFRD is larger than for WES2 for the 14 days (18–31 August) by 0.9 mm, with a standard deviation about the mean of 4.4 mm. (As an indication of the consistency of the measurements, with 15° minimum elevation angle the mean difference is 0.9 mm with a standard deviation of 3.9 mm. The standard deviation might be smaller for 15° minimum elevation angle for any of several factors, such as 1) increased smoothing of higher minimum elevation angle (fewer observations and weaker geometry); 2) seeing less anisotropy of the atmosphere; 3) smaller effect of scattering and multipath; or 4) smaller sensitivity to orbit errors. The height difference of 29 m from WFRD to WES2 would add 2.9 mm of ZWD for WES2 for an exponential scale height of 1500 m and the mean ZWD over the 15 days of approximately 150 mm. The standard deviation of the difference is comparable to the quadratic sum of the average formal uncertainties for ZWD for each site of 3.8 mm, but this
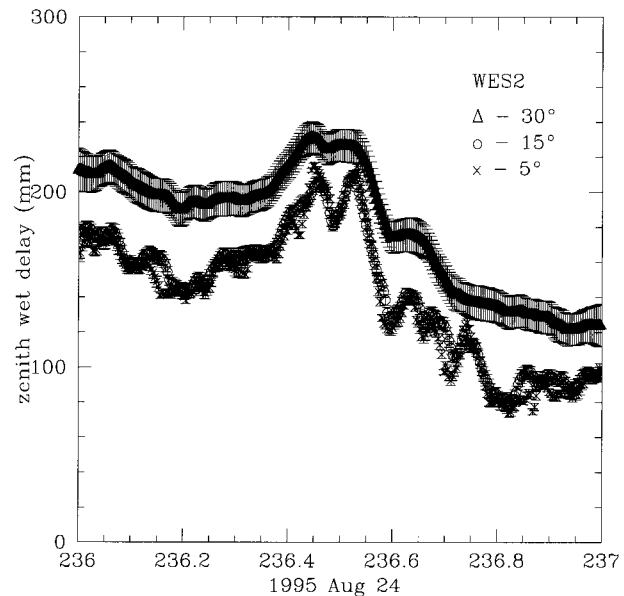


FIG. 11. ZWD estimates for the site WES2 for 24 Aug 1995 (DOY 236) for data included to a minimum elevation angle of 5° (× represents usually lowest trace), 15° (open square), and 30° (upper trace). The site positions were estimated in the same solution.

is not the correct assessment of the significance of the agreement for at least two reasons.

1) For each solution the chi-square per degree of freedom of the delay residuals is typically in the range 0.25 to 0.4, indicating that some component of the observation noise is too large by a factor of about two. The most likely candidate is the delay noise added to each observation (10 mm).
2) The atmosphere delays have been treated as uncorrelated at the three sites.

Any change in the ZWD estimates for a single site due to a variation in the analysis procedure sets a lower limit on the accuracy of the measurements. As discussed in section 4c, the estimates of ZWD and of GPS antenna height are correlated and depend on the minimum elevation angle of the data included in the solution. The estimates of ZWD for minimum elevations of 5°, 15°, and 30° for the site WES2 are shown in Fig. 11 for DOY 236. The effects of fewer observations and weaker geometry as the minimum elevation angle is increased are seen as a smoother variation with time of the ZWDs. Thus, raising the minimum elevation angle sacrifices precision in the estimation of ZWD. This may not be important if, for example, the observed ZWD cannot be assimilated at the higher rate by weather forecasters, or if the ZWD product does not contribute significantly to weather prediction. However, more importantly, the systematic change in average value as the minimum elevation angle is increased implies that the absolute value of ZWD cannot be determined by GPS unless an independent assessment of the correct minimum elevation
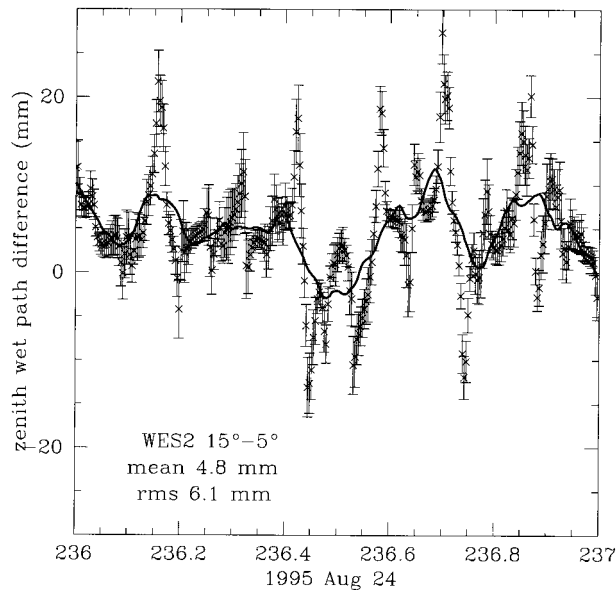
FIG. 12. The difference ZWD(15°) − ZWD(5°) for site WES2 for DOY 236 with site position estimated. The error bars are the quadratic difference of the uncertainties for the two elevations and represent the uncertainties in the differences. The smooth curve is a running boxcar average of 24 points, corresponding to 2 h of data.

TABLE 3. Scale factors and zero-point offsets for comparison of ZWD by different techniques. The relation is $A = aB + b$. The final column is the standard deviation of the $A$ values about the linear least squares solution.

| $A$ | $B$ | $a$ | $b$ (mm) | Std dev (mm) |
|---|---|---|---|---|
| VLBI(5°) | WVR | 0.93 ± 0.005 | 7.5 ± 0.6 | 6.5 |
| WES2(5°) | WVR | 0.95 ± 0.002 | 7.8 ± 0.3 | 6.6 |
| RS-80 | WVR | 0.91 ± 0.03 | 5 ± 4 | 6.7 |
| RS-80 | WES2(5°) | 0.94 ± 0.04 | −1 ± 5 | 10 |
| VLBI(5°) | WES2(5°) | 0.97 ± 0.005 | −0.7 ± 0.8 | 9.1 |

iable that may affect the accuracy of the ZWD estimates. The use of NMF as the mapping function may introduce deviations on a timescale of hours to days, but as discussed in section 3d and shown in Fig. 8, the VLBI estimates of ZWD do not exhibit any systematic dependence on minimum elevation. The average difference ZWD(VLBI) − ZWD(WVR) for the 4 days of VLBI data, after removing those points for which the WVR was affected by water on the optics, is −1 mm with a standard deviation of 7 mm. If the relation between the two is assumed to be linear, ZWD(VLBI) = $a$ZWD(WVR) + $b$, a least squares fit gives a scale factor of 0.93 ± 0.005 with an offset at zero of 8 ± 1 mm (Table 3). The large positive offset at zero, along with the scale factor of less than 1.0, combined with the limited range of ZWD, result in the apparently good agreement in terms of average difference.

By comparison, a linear fit of the GPS ZWD, using the results from WES2, to the WVR ZWD for the same time period, yields a relation of ZWD(WES2) = 0.95(±0.002) ZWD(WVR) + 7.8(±0.3) mm. The data are shown in Fig. 13. Although the mean value of the GPS ZWDs for 5° minimum elevation angle is 3 mm larger than the WVR values (interpolated to the time of the GPS measurements), this apparent close agreement is also fortuitous, since over the range of ZWD expe-

angle can be determined. Unfortunately this minimum elevation angle may not be the same for all systems since the local electromagnetic environment affects the elevation-angle dependence and differs for each location (Elósegui et al. 1995; Jaldehag et al. 1996b).

Unless either the elevation-angle dependence of the antenna response can be understood for each site, or the correct minimum elevation angle can be determined by comparison with an independent technique, GPS does not provide an absolute measure of ZWD comparable to the other techniques. There is also an impact on the precision of measurements. Since the estimated ZWD depends on the lowest observed elevation, the value will depend on the GPS satellite constellation at the time of each observation. The differences in ZWD estimates by WES2 for minimum elevations of 15° and 5° for DOY 236 are shown in Fig. 12. The solid line is a 2-h boxcar smoothing of the 300-s points to simulate the variation in the error that might be reported for use in numerical weather prediction. Differences in changes of ZWD of up to 25 mm of ZWD (∼4 mm of PWV) are evident, depending on the minimum elevation angle of the analysis. This is not to be confused with the bias that may exist between solutions with different minimum elevations. This is a difference in the change in ZWD with time, due to the elevation-angle dependence of the antenna and the elevation-angle distribution of the satellites in view.

### b. Comparison of WVR, GPS, and VLBI ZWD

For the analysis of the VLBI data, as for the GPS data, the minimum elevation angle is the primary var-
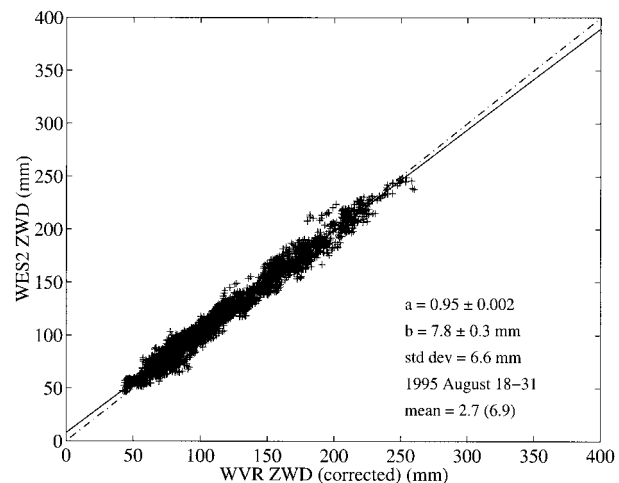


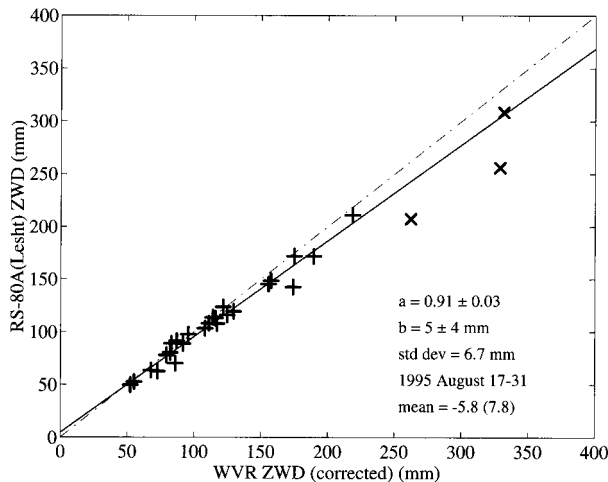FIG. 13. Comparison of ZWD by WES2 GPS with ZWD by WVR for 14 days (18–31 Aug 1995).

FIG. 14. Comparison of ZWD measured by radiosonde at the Haystack Observatory with ZWD measured by a WVR approximately 625 m away. The WVR values have been corrected to agree with the wet refractivity formulation of the GPS, VLBI, and radiosonde, as described in the text.

rienced during these observations the difference is not constant, but is a function of the total amount of water vapor.

A scale factor between the WVR ZWDs and the other techniques would not be unexpected since there is an uncertainty in the WVR results of approximately 5% that is proportional to the amount of water vapor present (section 3b). The scale uncertainty in both the VLBI and GPS measurements is ~1%, but this error is common to the two since it is due to the uncertainties in the refractivity coefficients of the water vapor and to the mapping functions. Thus the WVR data are consistent with the VLBI data and with the GPS data when using a 5° minimum elevation.

Although the comparisons with the GPS have been made using only the WES2 results, scale factors between pairs of GPS systems range from 0.98 to 1.02. Average ZWD differences between GPS sites for 5° minimum elevation angle agree within 3 mm after correction for height above sea level, as described above.

### c. Comparison of radiosonde ZWD measurements

In order to compare the GPS and WVR measurements with the radiosonde ZWD at approximately the same time, the values for 30 min following the radiosonde launch time were averaged. A comparison of the WVR and the corrected radiosonde data is shown in Fig. 14. Excluding the three values for which the WVR ZWD is greater than 250 mm (since the measurements occur at times when the WVR data might be contaminated by rain in spite of the attempt to remove such cases), the Vaisala RS-80 ZWD values are $0.91 \pm 0.03$ times the WVR ZWD values with a zero-point offset of $5 \pm 4$ mm. The RS-80 measurements are also $6\% \pm 4\%$ low

relative to the WES2 GPS data. Thus, even after correction for the contamination, the Vaisala A-HUMICAP® sensor appears to measure dry. Since relative humidity exceeded 80% on only a few days during this extremely dry period, it is not just for high humidities that the values are too low.

The accuracy of ZWD as measured by the WVR depends on the accuracy of the radiosonde data used to determine the retrieval coefficients. The WVR values reported here were determined using retrieval coefficients obtained from VIZ sondes analyzed by the NWS. As discussed in section 3b, the difference could lead to an error of up to 4% in comparing with the Vaisala RS-80 measurements.

### 6. Summary and discussion

Collocated measurements of ZWD were made by GPS, VLBI, WVR, and radiosonde during a 2-week period (only 4 days of VLBI) in August 1995. Additional GPS receivers covered a region of radius ~25 km. Before comparison could be made the WVR results required correction by −3.3% in order to use a definition of refractivity consistent with the other techniques, and the Vaisala RS-80 A-HUMICAP® radiosondes required a correction for packaging contamination that depended on the age of the sonde.

The VLBI data are internally consistent at a level of 3% (comparing the scale of the 5° and 15° minimum elevation angle solutions), and the mean value of the data are independent of the stringent elevation-angle cutoff test over the range 5°–30°, with a variation of only 6 mm of ZWD peak-to-peak (standard deviation ~1.5 mm). Comparison between data from two VLBI antennas separated by 1.24 km (in October 1989) gives a standard deviation of less than 4 mm and a mean difference of 4 mm.

The scales of the VLBI and GPS measurements agree to better than 3%, but the GPS data show a strong sensitivity to the amount of data at low elevations. This is due to multipath and near-field scattering in the vicinity of the GPS antenna mount and to the inclusion of a radome on some antennas. Based on agreement with the VLBI data, it is essential to include the lowest elevation-angle data possible for the best accuracy.

After corrections the WVR data and the radiosonde data have scale differences relative to the VLBI and GPS that are about 5% high (WVR) and 5% low (radiosonde), although these are both within the expected uncertainties of the techniques. Over the relatively low range of water vapor encountered during this experiment (~50–250 mm of ZWD) agreement of better than 6 mm of ZWD (~1 mm of PWV) has been shown to be achievable among the measurements.

This study has revealed the importance of specifying sufficient detail about the instrumentation and analysis when approaching agreement of better than 5% and 1 mm of PWV. By comparing ZWD instead of PWV the

additional uncertainty associated with the conversion is avoided.

The techniques evaluated in this study are complementary and should be used together to evaluate the actual accuracy achieved by any technique. Since the WVR measures a different quantity (integrated brightness temperature rather than integrated refractivity), improved agreement among the techniques will indicate a better understanding of the physical state of atmosphere. The high spatial and temporal densities of GPS make the global and regional networks extremely valuable instruments for measuring changes in the atmosphere. Reduction of scattering and multipath error in GPS through better understanding of the antenna environment will provide analysis corrections or engineering advances that can enhance the system accuracy significantly.

While VLBI cannot provide the temporal or spatial density of GPS, the accuracy of the technique, the ability to reanalyze all of the data as models are improved, and the distribution of VLBI antennas over a wide range of climates makes the archive of ZWD measurements a potential additional source of important climate data.

Finally, the accuracy of all of the techniques can be improved by changes in current analysis procedures, application of known corrections, or implementation of new models.

Because of the central role radiosondes occupy in the meteorological program, including their use for calibration of WVRs, it is essential that known corrections, such as that available for the Vaisala HUMICAP sensors, be applied.

Water vapor radiometer retrieval coefficients have a small dependence on the accuracy of the radiosonde measurements. Consequently, their determination should be based on corrected radiosonde data. As the accuracy of all of the techniques improves it is important to consider modifying the algorithms to account for higher-order terms (see Fig. 5).

The formal uncertainties of ZWD measurements by VLBI can be improved by reducing the minimum elevation of data included, but with the present models the repeatability of site position (and thus in ZWD by inference) degrades for elevations below about 7° (MacMillan and Ma 1994). This is probably due at least partly to errors in the atmospheric mapping functions. Recently a new mapping function set that utilizes in situ data from predicted or analyzed numerical weather models has been developed that should provide better precision without loss of accuracy (Niell 2000). Implementation of this mapping function and lowering the minimum elevation to 5° should produce a measurable improvement.

Based on the data from this experiment, it appears that the accuracy of GPS measurements using Dorne–Margolin choke ring antennas can be improved by reducing the minimum elevation of data included in the solutions to less than 10°. This conclusion has been reached from similar comparisons by others (e.g., Bar-Sever et al. 1998). For those GPS antennas protected by a radome, a correction should be applied. The correction should be measured for the specific type of radome in use. Ideally, the phases should be corrected before analysis. Alternatively, a bias could be applied that is determined for the minimum elevation observed. Such a correction depends on the distribution of the observations in elevation, and any elevation-dependent weighting will further affect the bias that should be used. Additional improvement when using lower elevation data will be obtained by also incorporating the new mapping functions.

The primary limitation of this study is the brief duration, since seasonal effects are likely to plague all of the techniques at some level.

## REFERENCES

Alber, C., R. Ware, C. Rocken, and F. Solheim, 1997: GPS surveying with 1 mm precision using corrections for atmospheric slant path delay. *Geophys. Res. Lett.,* **24,** 1859–1862.

Bar-Sever, Y. E., P. M. Kroger, and J. A. Borjesson, 1998: Estimating horizontal gradients of tropospheric path delay with a single GPS receiver. *J. Geophys. Res.,* **103** (B3), 5019–5035.

Bevis, M., S. Businger, T. A. Herring, C. Rocken, R. A. Anthes, and R. H. Ware, 1992: GPS meteorology: Remote sensing of atmospheric water vapor using the Global Positioning System. *J. Geophys. Res.,* **97,** 15 787–15 801.

——, ——, S. Chiswell, T. A. Herring, R. A. Anthes, C. Rocken, and R. H. Ware, 1994: GPS meteorology: Mapping zenith wet delays onto precipitable water vapor. *J. Appl. Meteor.,* **33,** 379–386.

Businger, S., and Coauthors, 1996: The promise of GPS in atmospheric monitoring. *Bull. Amer. Meteor. Soc.,* **77,** 5–18.

Carter, W. E., A. E. E. Rogers, C. C. Counselmann III, and I. I. Shapiro, 1980: Comparison of geodetic and radio interferometric measurements of the Haystack-Westford base line vector. *J. Geophys. Res.,* **85** (B5), 2685–2687.

Chen, G., and T. A. Herring, 1997: Effects of atmospheric azimuthal asymmetry on the analysis of space geodetic data. *J. Geophys. Res.,* **102** (B9), 20 489–20 502.

Clark, T. A., and Coauthors, 1998: Earth rotation measurement yields valuable information about the dynamics of the earth system. *EOS, Trans. Amer. Geophys. Union,* **79,** 205, 209.

Collins, J. P., and R. B. Langley, 1999: Possible weighting schemes for GPS carrier phase observations in the presence of multipath. U.S. Army Corps of Engineers Topographic Engineering Center Contract Rep. DAAH04-96-C-0086/TCN 98151, 33 pp.

Cruz Pol, S. L., C. S. Ruf, and S. J. Keihm, 1998: Improved 20- to 32-GHz atmospheric absorption model. *Radio Sci.,* **33,** 1319–1333.

Davis, J. L., T. A. Herring, I. I. Shapiro, A. E. E. Rogers, and G. Elgered, 1985: Geodesy by radio interferometry: Effects of atmospheric modeling errors on estimates of baseline length. *Radio Sci.,* **20,** 1593–1607.

Elgered, G., 1993: Tropospheric radio-path delay from ground-based microwave radiometry. *Atmospheric Remote Sensing by Microwave Radiometry,* Michael A. Janssen, Ed., John Wiley and Sons, 215–258.

——, J. L. Davis, T. A. Herring, and I. I. Shapiro, 1991: Geodesy by radio interferometry: Water vapor radiometry for estimation of the wet delay. *J. Geophys. Res.,* **96,** 6541–6555.

Elósegui, P., J. L. Davis, R. T. K. Jaldehag, J. M. Johansson, A. E. Niell, and I. I. Shapiro, 1995: Geodesy using the global positioning system: The effects of signal scattering on estimates of site position. *J. Geophys. Res.,* **100,** 9921–9934.

Emardson, T. R., J. M. Johansson, and G. Elgered, 2000: The systematic behavior of water vapor estimates using four years of GPS observations. *IEEE Trans. Geosci. Remote Sens.,* **38,** 324–329.

England, M. N., F. J. Schmidlin, and J. M. Johansson, 1993: Atmospheric moisture measurements: A microwave radiometer–radiosonde comparison. *IEEE Trans. Geosci. Remote Sens.,* **31,** 389–398.

Guo, Y.-R., Y.-H. Kuo, J. Dudhia, and D. Parsons, 1999: Four-dimensional variational data assimilation of heterogeneous mesoscale observations for a strong convective case. *Mon. Wea. Rev.,* **128,** 619–643.

Hauser, J. P., 1989: Effects of deviations from hydrostatic equilibrium on atmospheric corrections to satellite and lunar laser range measurements. *J. Geophys. Res.,* **94,** 10 182–10 186.

Herring, T. A., 1992: Submillimeter horizontal position determination using very long baseline interferometry. *J. Geophys. Res.,* **97,** 1981–1990.

——, J. L. Davis, and I. I. Shapiro, 1990: Geodesy by radio interferometry: The application of Kalman filtering to the analysis of very long baseline interferometry data. *J. Geophys. Res.,* **95,** 12 561–12 581.

Jaldehag, R. T. K., J. M. Johansson, J. L. Davis, and P. Elósegui, 1996a: Geodesy using the Swedish permanent GPS network: Effects of snow accumulation on estimates of site position. *Geophys. Res. Lett.,* **23,** 1601–1604.

——, ——, P. Elósegui, J. L. Davis, A. E. Niell, B. O. Rönnang, and I. I. Shapiro, 1996b: Geodesy using the Swedish permanent GPS network: Effects of signal scattering on estimates of relative site positions. *J. Geophys. Res.,* **101,** 17 814–17 860.

Kuo, Y.-H., Y.-R. Guo, and E. R. Westwater, 1993: Assimilation of precipitable water measurements into mesoscale numerical models. *Mon. Wea. Rev.,* **121,** 1215–1238.

Lanyi, G., 1984: Tropospheric delay effects in radio interferometry. TDA Progress Rep. 42-78, April–June 1984, Jet Propulsion Laboratory, Pasadena, CA, 37 pp. (The sign of Fbend4 was misprinted in this paper.)

Liljegren, J., B. Lesht, T. VanHove, and C. Rocken, cited 1999: A comparison of integrated water vapor from microwave radiometer, balloon-borne sounding system and Global Positioning System. *Proc. Ninth Atmospheric Radiation Measurement Program Science Team Meeting,* San Antonio, TX, ARM Program, 8 pp. [Available online at www.arm.gov/docs/documents/technical/conf_9903/liljegren(3)-99.pdf.]

MacMillan, D. S., 1995: Atmospheric gradients from very long baseline interferometry observations. *Geophys. Res. Lett.,* **22** (9), 1041–1044.

——, and C. Ma, 1994: Evaluation of very long baseline interferometry atmospheric modeling improvements. *J. Geophys. Res.,* **99,** 637–651.

Mendes, V. B., 1999: Modeling the neutral-atmosphere propagation delay in radiometric space techniques, Ph.D. dissertation, Department of Geodesy and Geomatics, Engineering Tech. Rep. 199, University of New Brunswick, Fredericton, New Brunswick, Canada, 353 pp.

Nash, J., and F. J. Schmidlin, 1987: WMO international radiosonde intercomparison (U.K., 1984; U.S.A., 1985) final report. World Meteorological Organization, Instruments and Observing Methods Rep. 30, WMO/TD-No. 195.

Niell, A. E., 1996: Global mapping functions for the atmosphere delay at radio wavelengths. *J. Geophys. Res.,* **101,** 3227–3246.

——, 2000: Improved atmospheric mapping functions for VLBI and GPS. *Earth, Planets, Space,* **52,** 699–702.

——, R. W. King, S. C. McClusky, and T. A. Herring, 1996: Radome effects on GPS height measurements with choke-ring antennas. *EOS, Trans. Amer. Geophys. Union,* May, p. S70.

Rocken, C., and Coauthors, 1995a: UNAVCO Academic Research Infrastructure (ARI) Receiver and Antenna Test Rep., 134 pp.

——, T. Van Hove, J. Johnson, F. Solheim, and R. Ware, 1995b: GPS/STORM–GPS sensing of atmospheric water vapor for meteorology. *J. Atmos. Oceanic Technol.,* **12,** 468–478.

Saastamoinen, J., 1972: Atmospheric correction for the troposphere and stratosphere in radio ranging of satellites. *The Use of Artificial Satellites for Geodesy, Geophys. Monogr.,* Vol. 15, Amer. Geophys. Union, 247–251.

Schroeder, J. A., and E. R. Westwater, 1991: Users' guide to WPL microwave radiative transfer software. NOAA Tech. Memo. ERL WPL-213, NOAA Wave Propagation Laboratory, Boulder, CO, 84 pp.

Schupler, B. R., T. A. Clark, and R. L. Allshouse, 1994: Signal characteristics of GPS user antennas. *Navigation,* **41** (3), 277–295.

Solheim, F. S., 1993: Use of pointed water vapor radiometer observations to improve vertical GPS surveying accuracy. Ph.D. dissertation, Department of Physics, University of Colorado, 128 pp.

——, J. Godwin, E. Westwater, Y. Han, S. Keihm, K. Marsh, and R. Ware, 1998: Radiometric profiling of temperature, water vapor, and cloud liquid water with various inversion methods. *Radio Sci.,* **33,** 393–404.

Staelin, D. H., 1966: Measurement and interpretation of the micro-

wave spectrum of the terrestrial atmosphere near 1-centimeter wavelength. *J. Geophys. Res.,* **71,** 2875–2881.

Treuhaft, R. N., and G. E. Lanyi, 1987: The effect of the dynamic wet troposphere on radio interferometric measurements. *Radio Sci.,* **22,** 251–265.

Wade, C. G., 1994: An evaluation of problems affecting the measurement of low relative humidity on the United States radiosonde. *J. Atmos. Oceanic Technol.,* **11,** 687–700.

——, and B. Schwartz, 1993: Radiosonde humidity observations near saturation. Preprints, *Eighth Symp. on Meteorological Observations and Instrumentation,* Anaheim, CA, Amer. Meteor. Soc., 44–49.

Wallace, J. M., and P. V. Hobbs, 1977: *Atmospheric Science: An Introductory Survey.* Academic Press, 350 pp.

Webb, F. H., and J. F. Zumberge, 1995: An introduction to GIPSY/OASIS-II. Tech. Rep. JPL-D-11088, California Institute of Technology, Pasadena, CA.

Wessel, P., and W. H. F. Smith, 1995: New version of the Generic Mapping Tools released. *EOS, Trans. Amer. Geophys. Union,* **76,** 329. [Available online at http://www.agu.org/eos_elec.]

Westwater, E. R., 1997: Remote sensing of tropospheric temperature and water vapor by integrated observing systems. *Bull. Amer. Meteor. Soc.,* **78,** 1991–2006.

——, M. J. Falls, and I. A. Popa Fatinga, 1989: Ground-based microwave radiometric observations of precipitable water vapor: A comparison with ground truth from two radiosonde observing systems. *J. Atmos. Oceanic Technol.,* **6,** 724–730.

——, and Coauthors, 1999: Ground-based remote sensor observations during PROBE in the tropical western Pacific. *Bull. Amer. Meteor. Soc.,* **80,** 257–270.

Zumberge, J. F., M. B. Heflin, D. C. Jefferson, M. M. Watkins, and F. H. Webb, 1997: Point positioning for the efficient and robust analysis of GPS data from large networks. *J. Geophys. Res.,* **102,** 5005–5017.